Tunable Spin Loading and T_{1} of a Silicon Spin Qubit Measured by Single-Shot Readout

C. B. Simmons, J. R. Prance, B. J. Van Bael, Teck Seng Koh, Zhan Shi, D. E. Savage, M. G. Lagally, R. Joynt, Mark Friesen, S. N. Coppersmith, and M. A. Eriksson

Tunable spin loading and T_1 of a silicon spin qubit measured by single-shot readout

C. B. Simmons, J. R. Prance, B. J. Van Bael, Teck Seng Koh, Zhan Shi, D. E. Savage,
M. G. Lagally, R. Joynt, Mark Friesen, S. N. Coppersmith, and M. A. Eriksson
Department of Physics, University of Wisconsin-Madison, Madison, WI 53706, USA

We demonstrate single-shot readout of a silicon quantum dot spin qubit, and we measure the spin relaxation time T_1. We show that the rate of spin loading can be tuned by an order of magnitude by changing the amplitude of a pulsed gate voltage, and the fraction of spin-up electrons loaded can also be controlled. This tunability arises because electron spins can be loaded through an orbital excited state. Using theory that includes excited states of the dot and energy dependent tunneling, we find that a global fit to the loading rate and spin-up fraction is in good agreement with the data.

The properties of silicon have made it the central material for the fabrication of current microelectronic devices. Silicon's fundamental properties also make it an attractive option for the development of devices for spintronics [1] and quantum information processing (QIP) [2–5]. Spin qubits in silicon are expected to have long coherence times, thanks to the predominance of a spin-zero nuclear isotope and relatively weak spin-orbit coupling. However, silicon quantum dots have yet to demonstrate the reproducibility and controllability achieved in gallium arsenide devices [6–9]. In particular, the ability to manipulate and measure spins of single electrons is crucial for applications in spintronics and QIP. Spin relaxation times in Si quantum dots have been measured using time-averaged techniques [10, 11]. Readout of spin qubits requires single-shot spin measurement [12, 13], something that has not been demonstrated in gate-defined Si quantum dots. Gated quantum dots are important for QIP, because they are highly tunable, and the demonstration of qubits in double [6] and triple [14] quantum dots offers a path towards scalability. Further, tunability enables control over coupling to both ground and excited states, which has the potential to enable rapid qubit initialization.

In this Letter, we demonstrate single-shot spin readout in a silicon quantum dot spin qubit, and we report single-shot measurement of the longitudinal spin relaxation time T_1. We further demonstrate that the rate of loading of electron spins can be tuned over an order of magnitude using a gate voltage, that the spin state depends systematically on the loading voltage level, and that this tunability arises because electron spins can be loaded through excited orbital states of the quantum dot. The longitudinal spin relaxation time T_1 is found to be ~ 3 seconds at a field of 1.85 Tesla. The demonstration of single spin measurement as well as a long spin relaxation time and tunability of the loading are all favorable properties for spintronics and quantum information processing applications. Our results show that Si/SiGe quantum dots can be fabricated that are sufficiently tunable to enable single-electron manipulation and measurement, and
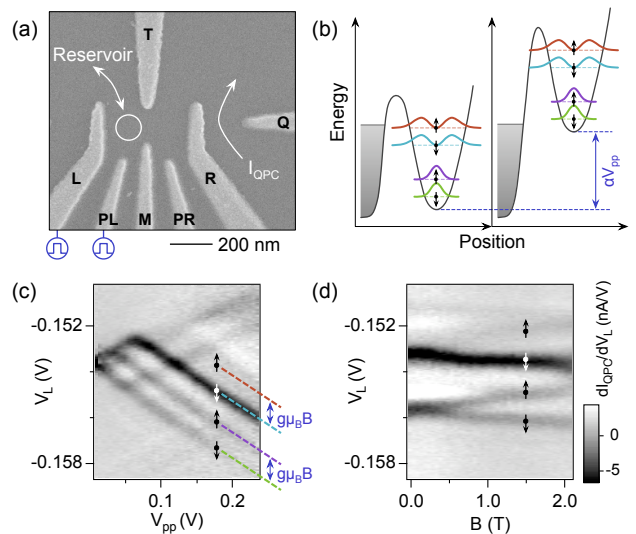

FIG. 1: (a) Scanning electron micrograph of a device identical to that used here. The gates are tuned so that a single quantum dot exists at the location of the white circle and tunneling occurs to and from the left reservoir only. Charge sensing is performed by measuring the current I_{QPC}. (b) Voltage pulses of amplitude V_{PP}, applied to either gate L or PL, adjust the energy levels of the dot. The case shown corresponds to loading an electron during the positive phase of the pulse (left) through any of the four states $| \downarrow g \rangle, | \uparrow g \rangle, | \downarrow e \rangle, | \uparrow e \rangle$ that are below the Fermi energy E_F, and then unloading the electron during the negative phase of the pulse (right). (c) & (d) Measurements of dI_{QPC}/dV_L, in the presence of a pulsed voltage V_{PP} on gate L. Transitions to the three lowest eigenstates, $| \downarrow g \rangle, | \uparrow g \rangle$, and $| \downarrow e \rangle$, are clearly visible in (c), where the magnetic field $B = 1.5$ T. The state $| \uparrow e \rangle$ is expected at the location shown by the red dashed line but is invisible due to the strong coupling of the excited state $|e\rangle$. As a function of B (and with $V_{PP} = 0.125$ V), the ground and first orbital excited states split linearly due to the Zeeman effect.

that long spin relaxation times are consistent with the orbital and/or valley excitation energies in these systems.

The measurements we report were performed in a dilution refrigerator with a parallel magnetic field on a gate-defined quantum dot fabricated from a Si/SiGe het-

erostructure, using the methods outlined in Ref. [15]. The gate configuration is shown in Fig. 1(a), and the gates were tuned so that the device was in the few-electron, single-dot regime. The electron temperature was 143 ± 10 mK, measured by fitting the width of electronic transitions as the base temperature of the dilution refrigerator was raised.

As shown in Fig. 1(b), an electron can be loaded into one of four energy eigenstates; we denote the states, in order of increasing energy, as $|\downarrow g\rangle$, $|\uparrow g\rangle$, $|\downarrow e\rangle$, and $|\uparrow e\rangle$, where the first index refers to spin ($\downarrow$ having lower energy than $\uparrow$) and the second to the ground (g) and excited (e) orbital levels. We obtain an experimental map of the discrete energy spectrum by measuring the differential current dI_{QPC}/dV_L through a charge sensing quantum point contact while applying square voltage pulses to gate L. The grayscale plots of dI_{QPC}/dV_L in Fig. 1(c,d) reveal dark lines corresponding to the onset of tunneling to the energy eigenstates when the transitions come into resonance with the Fermi energy E_F [16]. The measured calibration factor for gate L, $\alpha = 0.125 \pm 0.006$ eV/V, translates the positions of these lines into a spectroscopy of the dot energy levels.

In Fig. 1(c), the darkest line indicates the onset of transitions to the orbital excited state $|e\rangle$ of energy $311 \pm 19\,\mu$eV. This relatively large energy splitting is favorable for applications in which spin coherence is desirable [17], and it is notable because the low-lying excited orbital states in Si/SiGe quantum dots have fundamental differences compared to those in GaAs [18], because of the role of valley degrees of freedom [19–25]. The Zeeman splitting of the ground and excited states is shown in Fig. 1(d).

A main focus of this work is to demonstrate that orbital excited states can be exploited to control both the rate of loading and the spin state of the electron loaded into the dot. To measure the spin state of individual electrons, we use a 3-level pulsed-gate technique for single-shot readout pioneered in Ref. [12]. Starting with the electron unloaded, V_{PL} is rapidly changed to a load level. A downward step is visible in I_{QPC} during the load stage when an electron of either spin tunnels onto the dot. V_{PL} is then changed to the readout level. During the readout stage, a spin-$\uparrow$ electron can tunnel off the dot, and a spin-$\downarrow$ electron will tunnel on to replace it, resulting in a pulse in I_{QPC} that persists as long as the dot is unloaded. In contrast, a spin-$\downarrow$ electron will remain in the dot and no current pulse will occur during the readout phase. During the final, empty stage, the electron tunnels off the dot regardless of its spin orientation.

Three single-shot spin readout traces are shown in Fig. 2(a–c). In each case, the voltage levels for the readout and empty stages are the same. As shown in the schematics, the load level is varied for preferential loading of states $|\uparrow g\rangle$, $|\downarrow e\rangle$, and $|\uparrow e\rangle$ in panels (a), (b), and (c), respectively. The data in (a) and (c) show that
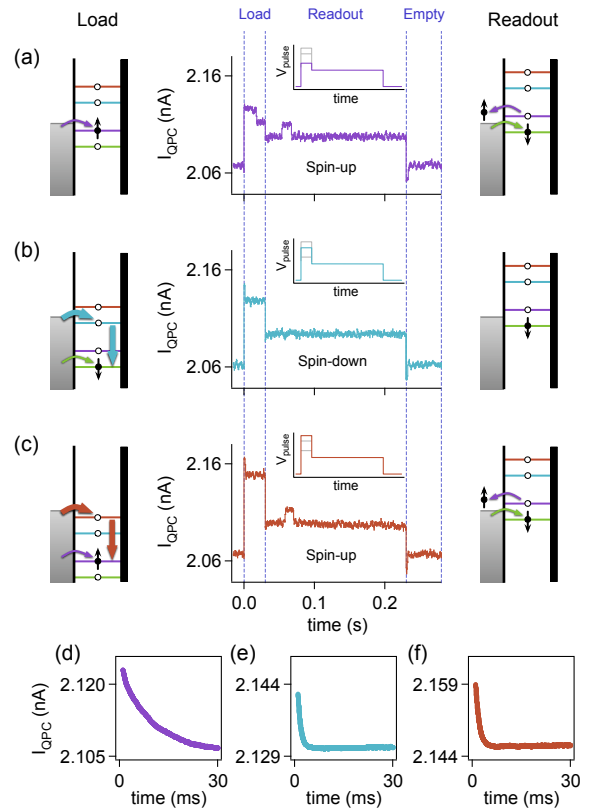

FIG. 2: A 3-level gate voltage pulse sequence consisting of load, readout and empty stages is applied to gate PL for single-shot spin readout. The loading rate and the probability for loading different spin states vary with the loading voltage level. Panels (a), (b), (c) correspond respectively to preferential loading of states $|\uparrow g\rangle$, $|\downarrow e\rangle$, and $|\uparrow e\rangle$ at load voltages $V_{\mathrm{load}} = +175, +325$, and $+425$ mV. The single-shot traces in (a) and (c) are identified as spin-$\uparrow$ because of the current pulse during readout caused by a spin-$\uparrow$ tunneling off the dot and a spin-$\downarrow$ replacing it. Trace (b), which has no such pulse, is identified as spin-$\downarrow$. The schematics indicate the possible loading channels for each case. For all cases: $t_{\mathrm{load}} = 30$ ms, $t_{\mathrm{readout}} = 200$ ms, $V_{\mathrm{readout}} = +75$ mV, $t_{\mathrm{empty}} = 50$ ms, and $V_{\mathrm{empty}} = -200$ mV. (d), (e), (f) Average of 500 time traces of electron loading events for the load voltages of panels (a), (b), and (c), respectively. Loading at the excited orbital state (shown in both (e) and (f), with tunnel rates of 1186 ± 3Hz and 958 ± 2Hz, respectively), is much faster than loading at the ground state (shown in (d), with a tunnel rate of 106.7 ± 0.2 Hz). The tunnel rates and uncertainties come from exponential fits.

a spin-$\uparrow$ was loaded, and the data in (b) show that a spin-$\downarrow$ was loaded. The loading rate can be determined by averaging many loading events together, resulting in an exponential decay of I_{QPC} from a magnitude corresponding to an unloaded electron to that corresponding to a loaded electron. Panels (d–f) show that the loading rates into the excited orbital states are much faster than into the ground orbital states.

The rate at which an electron loads into the dot, as well

as the spin state of that electron, both depend strongly on the voltage at which the electron is loaded. In Fig. 3, we show that these features are observed over a wide range in gate voltage. Fig. 3(a) shows that the loading rate Γ_{load}, measured in the same way as in Fig. 2(d–f), but now as a continuous function of loading level, increases by over an order of magnitude when the electron is loaded through an orbital excited state instead of through the orbital ground state. The loading rate shows two strong peaks as a function of loading voltage, corresponding to the excited states $|\uparrow e\rangle$ and $|\downarrow e\rangle$. Because orbital relaxation is very fast compared to the experimental time scale [26, 27], one expects any electron loaded into a spin-$\uparrow$ state to be measured in the state $|\uparrow g\rangle$, and any electron loaded into a spin-$\downarrow$ state is measured in the state $|\downarrow g\rangle$.

The relative fraction of spin-$\uparrow$ and spin-$\downarrow$ loaded can be tuned, because the loading rate for each spin type is voltage dependent. We demonstrate this directly by using single-shot spin readout to measure the spin-$\uparrow$ fraction as a function of the loading level, as shown in Fig. 3(b). The fraction of spin-$\uparrow$ electrons has two clear peaks as a function of the loading voltage, one corresponding to $|\uparrow g\rangle$ and a second to $|\uparrow e\rangle$. These peaks arise because loading rates into specific spin states in the dot are a maximum when the state is near resonance with the Fermi level.

The variation in both the total loading rate and the spin-$\uparrow$ fraction can be understood by calculating the loading rate for each spin state. The probability of loading a spin-$\uparrow$ electron is $\Gamma_\uparrow/\Gamma_{\text{load}}$, where $\Gamma_\uparrow$ is the total rate for all spin-$\uparrow$ channels, and Γ_{load} is the sum of the rates for all ways to load the dot. A global fit to the data in terms of loading through spin-split ground and excited states with Lorentzian broadening is shown in Fig. 3(a) and (b). The fit is to both the total loading rate and the fraction of spin-$\uparrow$ electrons. We treat the loading rate contribution from each state as a convolution of a Fermi-Dirac distribution, a Lorentzian lineshape, and a linearized energy dependent tunneling function [28]:

$$\Gamma_i(V) = \int_{-\infty}^{\infty} \left(\frac{\Gamma_{0i} e^{-\alpha y/E_i}}{1 + e^{-\alpha y/k_B T}} \right) \frac{\gamma_i/2\pi}{(\gamma_i/2)^2 + (\delta V_i - y)^2} dy,$$

(1)

where E_i is the linearized energy dependent tunneling coefficient that relates to the transparency of the barrier [29]; γ_i is the full width at half maximum of the Lorentzian; Γ_{0i} is the amplitude; V is the loading voltage; and $\delta V_i = V - V_i$, where V_i is the position of the state (see EPAPS Document for additional details). The fit is in good agreement with the experimental measurements for the loading rates and the fractions of spin-$\uparrow$ and spin-$\downarrow$ electrons, supporting the interpretation of the data in terms of loading through specific spin states of the dot.

The black line in Fig. 3(b) is corrected for the finite spin lifetime T_1 of the electrons loaded into the dot. We determine T_1 by measuring the spin-$\uparrow$ fraction as a func-
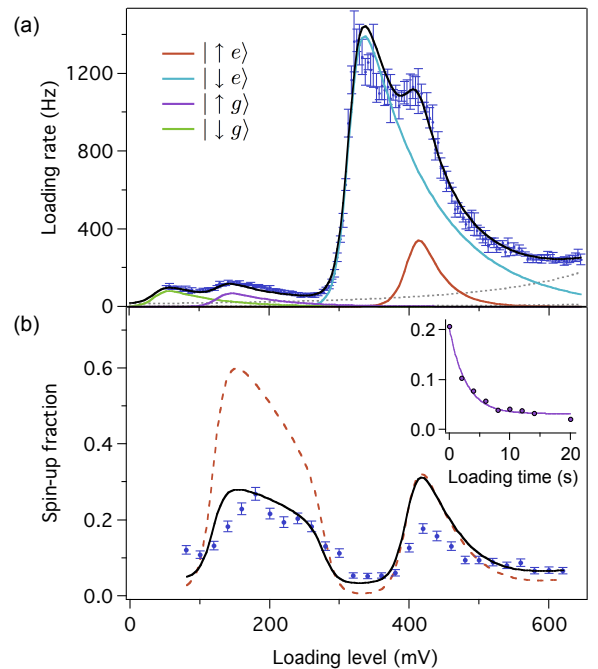

FIG. 3: Spin selective loading and spin lifetime measurement. (a) Plot of electron loading rate Γ_{load} versus loading voltage V_{load} on gate PL at $B = 1.85$ T. Error bars are the standard deviation of four measurements. Peaks occur when levels in the dot are made available for loading, enabling tuning of both the loaded-spin fraction and the loading rate. The spin-split excited orbital levels $|\uparrow e\rangle$ and $|\downarrow e\rangle$ load ~ 10 times faster than the ground state. The black solid line in (a) is a fit obtained by treating the loading rate contribution from each state as a convolution of a Fermi-Dirac distribution, Lorentzian lineshape, and a linearized energy dependent tunneling function. (b) Spin-up fraction versus loading level measured using single-shot readout (see Fig. 2), with $t_{\text{load}} = 100$ ms, $t_{\text{readout}} = 200$ ms, $t_{\text{empty}} = 50$ ms, $V_{\text{readout}} = +85$ mV and $V_{\text{empty}} = -200$ mV. Each data point corresponds to an analysis of 1000 single-shot traces. The red dashed line is a fit using the same parameters as in (a); the black solid line is the same fit with corrections for the T_1 decay before measurement, a measurement fidelity less than unity, and a non-zero dark count rate. Error bars are $\sqrt{M}$, where M is the number of readout events. Inset: Spin-up fraction versus loading time with $V_{\text{load}} = +425$ mV. The solid line is an exponential fit that yields $T_1 = 2.8 \pm 0.3$ s.

tion of the duration of the loading pulse, t_{load} [12]. The inset of Fig. 3(b) shows a typical result for a magnetic field of 1.85 T, with an exponential fit yielding the value $T_1 = 2.8 \pm 0.3$ s. For these data, $V_{\text{load}} = +425$ mV, so that loading occurs predominantly through the excited orbital states. We have measured T_1 at different loading voltages and also measured T_1 for a four-step pulse sequence in which the dot is held at a fourth "wait" voltage. The values of T_1 were all of order seconds, except when both the "load" and "wait" voltages were set so the state $|\uparrow g\rangle$ was aligned just below E_F, where the value

of T_1 is reproducibly much shorter: $T_1 = 136 \pm 22$ ms. In principle, virtual hopping of electrons from the dot to the leads can limit T_1 [30], but the predicted magnitude is much too small to explain the observed effect, and this mechanism is not consistent with the behavior when the "wait" voltage is varied. The possibility that the excited orbital states are long-lived is ruled out by performing single-shot measurement with the readout level positioned such that $| \downarrow g \rangle$ and $| \uparrow g \rangle$ are below E_F and $| \downarrow e \rangle$ and $| \uparrow e \rangle$ are above E_F. In this situation, even for short loading times ($t_{\text{load}} = 20$ ms), less than 0.5% of traces show events.

It has been observed that T_1 can be limited by dipolar coupling to nearby spins [13]; we believe that the shorter T_1 time measured when the dot is loaded through the state $| \uparrow g \rangle$ is due to interaction with a nearby spin trap, which is suppressed by the deeper pulse associated with loading at the excited orbital states. The ability to load an electron into the dot through the excited state thus provides an immediate benefit, in that the additional tunability enables one to avoid sample imperfections that lead to a shorter spin relaxation time.

We have demonstrated the ability to manipulate and measure the spin state of individual electrons in a Si/SiGe quantum dot, and we report the first single-shot measurements of the longitudinal spin relaxation time T_1 in such devices. We have shown that loading into spin-split orbital excited states provides a fast channel for initializing spins into the ground orbital spin qubit states because of the coexistence of fast orbital relaxation and slow spin relaxation. The demonstrations of fast initialization and slow spin relaxation enhance the prospects for the development of Si/SiGe devices for spintronics and quantum information processing applications.

An EPAPS Document contains a description of the identification of loading and unloading events using a wavelet technique, details of the peak fitting in Fig. 3, and additional details of the experimental measurements.

[1] I. Appelbaum, B. Huang, and D. Monsma, Nature **447**, 295 (2007).

[2] B. E. Kane, Nature **393**, 133 (1998).

[3] D. Loss and D. P. DiVincenzo, Phys. Rev. A **57**, 120 (1998).

[4] R. Vrijen, E. Yablonovitch, K. Wang, H. W. Jiang, A. Balandin, et al., Phys. Rev. A **62**, 012306 (2000).

[5] M. Friesen, P. Rugheimer, D. E. Savage, M. G. Lagally, D. W. van der Weide, et al., Phys. Rev. B **67**, 121301 (2003).

[6] J. R. Petta, A. C. Johnson, J. M. Taylor, E. A. Laird, A. Yacoby, et al., Science **309**, 2180 (2005).

[7] F. H. L. Koppens, C. Buizert, K. J. Tielrooij, I. T. Vink, K. C. Nowack, et al., Nature **442**, 766 (2006).

[8] M. Pioro-Ladrière, T. Obata, Y. Tokura, Y.-S. Shin, T. Kubo, et al., Nat. Phys. **4**, 776 (2008).

[9] S. Amasha, K. MacLean, I. P. Radu, D. M. Zumbühl, M. A. Kastner, et al., Phys. Rev. B **78**, 041306 (2008).

[10] M. Xiao, M. G. House, and H. W. Jiang, Phys. Rev. Lett. **104**, 096801 (2010).

[11] R. R. Hayes, A. A. Kiselev, M. G. Borselli, S. S. Bui, E. T. Croke III, et al. (2009), arXiv: 0908.0173v1.

[12] J. M. Elzerman, R. Hanson, L. H. W. van Beveren, B. Witkamp, L. M. K. Vandersypen, et al., Nature **430**, 431 (2004).

[13] A. Morello, J. Pla, F. Zwanenburg, K. Chan, K. Tan, et al., Nature **467**, 687 (2010).

[14] E. A. Laird, J. M. Taylor, D. P. DiVincenzo, C. M. Marcus, M. P. Hanson, et al., Phys Rev B **82**, 075403 (2010).

[15] M. Thalakulam, C. B. Simmons, B. M. Rosemeyer, D. E. Savage, M. G. Lagally, et al., Appl. Phys. Lett. **96**, 183104 (2010).

[16] J. M. Elzerman, R. Hanson, L. H. W. van Beveren, L. M. K. Vandersypen, and L. P. Kouwenhoven, Appl. Phys. Lett. **84**, 4617 (2004).

[17] C. Tahan, M. Friesen, and R. Joynt, Phys. Rev. B **66**, 035314 (2002).

[18] R. Hanson, L. P. Kouwenhoven, J. R. Petta, S. Tarucha, and L. M. K. Vandersypen, Rev. Mod. Phys. **79**, 1217 (2007).

[19] T. B. Boykin, G. Klimeck, M. A. Eriksson, M. Friesen, S. N. Coppersmith, et al., Appl. Phys. Lett. **84**, 115 (2004).

[20] S. Goswami, K. A. Slinker, M. Friesen, L. M. McGuire, J. L. Truitt, et al., Nat. Phys. **3**, 41 (2007).

[21] N. Kharche, M. Prada, T. B. Boykin, and G. Klimeck, Appl. Phys. Lett. **90**, 092109 (2007).

[22] G. P. Lansbergen, R. Rahman, C. J. Wellard, I. Woo, J. Caro, et al., Nat. Phys. **4**, 656 (2008).

[23] D. Culcer, L. Cywinski, Q. Z. Li, X. Hu, and S. Das Sarma, Phys. Rev. B **80**, 205302 (2009).

[24] M. Friesen and S. N. Coppersmith, Phys. Rev. B **81**, 115324 (2010).

[25] M. Fuechsle, S. Mahapatra, F. A. Zwanenburg, M. Friesen, M. A. Eriksson, et al., Nat. Nanotechnol. **5**, 502 (2010).

[26] A. Khaetskii and Y. Nazarov, Phys. Rev. B **61**, 12639 (2000).

[27] M. Friesen, C. Tahan, R. Joynt, and M. A. Eriksson, Phys. Rev. Lett. **92**, 037901 (2004).

[28] S. Datta, *Electronic Transport in Mesoscopic Systems* (Cambridge University Press, Cambridge, UK, 1995).

[29] K. MacLean, S. Amasha, I. P. Radu, D. M. Zumbühl, M. A. Kastner, et al., Phys. Rev. Lett. **98**, 036802 (2007).

[30] A. B. Vorontsov and M. G. Vavilov, Phys. Rev. Lett. **101**, 226805 (2008).